Revista Ciencia en Desarrollo. Vol. 16 Num. 2. pp. 191 - 203
julio - diciembre

DOI: 10.19053/uptc.01217488.v16.n2.2025.19052

Artículo de investigación

Controlled release of glyphosate supported/encapsulated on organoclays host and alginate over an amazon colombian soil column

Liberación controlada de glifosato soportado/encapsulado en organoarcillas y alginato sobre una columna de suelo amazónico colombiano

Angela María Cuellar-Felantana[1], Jaime Fernando Martínez-Suárez[1] and Lisette Ruiz-Bravo[1] ✉

[1]Programa de Química, Facultad de Ciencias Básicas, Universidad de la Amazonia, Florencia, Colombia.

Recepción: 26-marzo-2025 **Aceptado:** 07-junio-2025 **Publicado:** 20-julio-2025
Cómo citar: Cuellar-felantana, A. M., Martínez-Suárez, J. F., & Ruiz Bravo, L. (2025). Liberación controlada de glifosato soportado/encapsulado en organoarcillas y alginato sobre una columna de suelo amazónico colombiano. *Ciencia En Desarrollo*, 16(2).
doi: 10.19053/uptc.01217488.v16.n2.2025.19052

Abstract

Controlled release formulations (CRF) are implemented to modulate the concentration of the active ingredient provided to the soil over time. In this work, CRF of glyphosate previously supported on bentonite/organobentonite (host materials) and with alginate as encapsulating agent in different host material/alginate ratios were obtained to evaluate the desorption profile in water and soil columns. The results indicate that the organobentonite with a higher content of alkylammonium cations reaches glyphosate qs of up to 2.078 mg g^{-1} at pH 10, due to an ionic interaction between the negatively ionized glyphosate and its positive surface. The adsorption results best fit the Sips model indicating heterogeneity in the adsorption sites on the surface of the materials. The encapsulation of the glyphosate/organobentonite (OBGE) systems was carried out with alginate as a crosslinking agent using the extrusion technique, spherical encapsulates with particle sizes >2.3 mm was obtained. The water activity study showed activities < 0.6 suggesting the inhibition of the growth of microorganisms. The experiment of release glyphosate encapsulated in water were performed with the encapsulates containing glyphosate - host materials in different proportions (0.1 and 0.4) and reach a release between 25 – 35 %, with the encapsulated with lower ratio of glyphosate/organobentonite OBGE(0.1). These results were adjusted to the empirical model of Korsmeyer-Peppas which are related to controlled release profiles whose predominant mechanism is simple Fickian diffusion. The experiment in soil columns demonstrated that OBGE(0.1) slowly releases the active component through the soil profile compared to the commercial formulation.

Keywords: biopolymer matrix, herbicide release, encapsulation, organobentonite, slow-release formulation, cyclic voltammetry, copper electrode.

Resumen

Las formulaciones de liberación controlada (CRF) se implementan para modular la concentración del ingrediente activo suministrado al suelo a lo largo del tiempo. En este estudio, se obtuvieron CRF de glifosato previamente soportado en bentonita/organobentonita (materiales host) y encapsulado con alginato como agente encapsulante en diferentes relaciones material hospedador/alginato, con el objetivo de evaluar el perfil de desorción en agua y columnas de suelo. Los resultados indican que la organobentonita con un mayor contenido de cationes alquilamonio alcanza capacidades de adsorción de glifosato de hasta 2.078 mg g^{-1} a pH 10, debido a una interacción iónica entre el glifosato ionizado negativamente y la superficie cargada positivamente del material. Los datos de adsorción se ajustaron mejor al modelo de Sips, lo que sugiere heterogeneidad en los sitios de adsorción sobre la superficie de los materiales. La encapsulación de los sistemas glifosato/organobentonita (OBGE) se realizó utilizando alginato como agente reticulante mediante la técnica de extrusión, obteniéndose encapsulados esféricos con tamaños de partícula superiores a 2.3 mm. El estudio de actividad de agua mostró valores inferiores a 0.6, lo que sugiere la inhibición del crecimiento microbiano. Los experimentos de liberación de glifosato encapsulado en agua se llevaron a cabo con encapsulados que contenían glifosato y materiales hospedadores en diferentes proporciones (0.1 y 0.4), alcanzando una liberación entre el 25 y el 35 %, siendo la formulación OBGE(0.1) la de menor relación glifosato/organobentonita. Estos resultados se ajustaron al modelo empírico de Korsmeyer-Peppas, asociado a perfiles de liberación controlada donde el mecanismo predominante es la difusión Fickiana simple. El experimento en columnas de suelo demostró que OBGE(0.1) libera el ingrediente activo de manera más lenta a través del perfil del suelo en comparación con la formulación comercial.

Palabras Clave: Matriz biopolimérica, liberación de herbicidas, encapsulación, organobentonita, formulación de liberación lenta, voltamperometría cíclica, electrodo de cobre.

E-ISSN: 2462-7658

1 Introduction

Glyphosate (N-phosphonomethylglycine) is a broad-spectrum herbicide widely used in agriculture across South America [1, 2]. In Colombia, it has been used both in agro-industrial production [3, 4] and for the eradication of illicit crops [5, 6]. However, its use has become increasingly controversial due to environmental and health concerns. Since 2015, glyphosate has been banned or restricted in several countries, including Sri Lanka, Luxembourg, and parts of the European Union, due to its classification by the International Agency for Research on Cancer (IARC) as a probable human carcinogen (Group 2A) and its adverse effects on ecosystems and biota [7]. In Colombia, aerial spraying of glyphosate was banned in 2015 by the Constitutional Court (Ruling T-236/2017), primarily because of its environmental impact on biodiversity-rich and sensitive areas like the Amazon region [8, 9].

Despite these restrictions, glyphosate remains in use for terrestrial agricultural applications, and its persistence in the environment remains a major concern. In tropical ecosystems with heavy rainfall and high soil permeability, commercial formulations of glyphosate can be rapidly transported to surface and groundwater bodies through infiltration, runoff, and leaching [10, 11] and as a result polluting the environment [12]. The high water solubility of glyphosate, typically sold as a salt, exacerbates this mobility, especially when applications coincide with rainy periods [13]. Additionally, excessive application rates are often used to compensate for herbicide losses due to leaching, increasing the risk of environmental contamination. .

To address these issues, controlled release systems (CRS) have been proposed as an effective strategy to reduce the mobility and dosage of herbicides in the environment. These systems are designed to gradually release the active compound over time, maintaining efficacy while minimizing off-target effects [14]. Controlled release formulations typically involve the encapsulation or adsorption of the herbicide within polymeric or inorganic matrices, which protect the active ingredient from immediate leaching. Examples include bentonite [15], kaolinite [16], organoclays [17], and various synthetic polymers [18-21].

In the particular case of glyphosate controlled release systems, the technology has been developed on supports such as atapulgite clay that gradually releases glyphosate based on pH (Zha 2022), Mg-Al double-layer lamellar hydroxides, achieving the release of up to 50% of the herbicide after 5 hours [22] and hydroxides Zn-Al double-layer sheets with a reduction in the release of the active component of up to 50% in the range of 6.5 to 18.6 h [23]. However, materials imply high acquisition costs, so the use of alternative materials has been set as a point of special attention. Clay minerals, and especially bentonite, are easily accessible, have a ubiquitous presence in the soil, and have the appropriate characteristics for this use, since surface and interlayer adsorption of large organic molecules (such as those of glyphosate) through cation exchange reactions. In addition, they have been implemented as ecological modifications by providing great stability during the useful life of the products [24]. Bentonite has been modified or activated with large organic molecules in order to enhance the affinity of its surface, going from being hydrophilic in its natural form to hydrophobic when organic molecules such as alkylammonium cations are incorporated [25]. On the other hand, encapsulation with alginate is characterized by protecting the supply of the encapsulated compound while controlling its release through the modulation of desorption until the alginate membrane degrades [26].

The objective of this study was to obtain controlled release formulations of glyphosate, using organobentonite as host material and alginate as encapsulating agent in different host material/alginate ratios to evaluate the desorption profile in water and soil columns.

2 Experimental

2.1 Synthesis and characterization of host materials

The synthesis of organoclay (host material) was performed based on the procedure reported by [27]. Hexadecylamine (Sigma – Aldrich, 90%) equivalent to 1, 1.7 and 3 times the ion exchange capacity of bentonite of Valle del Cauca (80.5 meq/100 g clay, previously purified and characterized) was dissolved in 0.1 N HCl; the mixture was stirred at 80 °C in a water bath for 3 hours. Subsequently 2 g of clay was added and stirred for 3 hours, keeping the temperature at 80 °C. Then it was washed, mixed with 50 mL of water, and shaken for 30 minutes at 50 °C. Finally, it was centrifuged at 4500 r.p.m for 30 minutes and the precipitate was mixed with a water: ethanol mixture (1:1 v/v) at 50 °C and left in agitation during the whole night centrifuged again, discarding the supernatant and the solid was dried at room temperature. The materials obtained are named OB1, OB1.7 and OB3.

The host materials were characterized using XRD and FTIR. The solids were characterized by X-ray diffraction in a BRUKER model D8 ADVANCE diffractometer with DaVinci geometry. The diffractometer operated at 40 kV and 40 mA and is equipped with a divergent slit of 0.6 mm, a Cu $K_{\alpha 1}$ radiation source and a nickel filter. The measurements were taken from 2 to 15° 2θ using a step size of 0.02° 2θ and 0.4 s per step. FT-IR spectra were obtained with a Nicolet model IS50-Thermo Scientific spectrometer in a range between 4000 - 400 cm^{-1}, using KBr pellets.

2.2 Glyphosate quantification

2.2.1 Electrochemical determination

All voltammetry measurements were performed using potentiostat/galvanostat Metrohm 797 VA Computrace (Herisau, Switzerland) with Software Version 1.3.2. Cyclic Voltammetry (CV) experiments were performed in an undivided glass cell. Working electrode (WE) was a 3 mm diameter copper disk encapsulated in Teflon, auxiliary electrode (AE) was a Pt rod, and Ag/AgCl with double junction was used as a reference electrode. Glyphosate calibration curve was performed by CV. CV was recorded over a potential range from 400 mV to -400 mV at a sweep rate of 100 mV s^{-1}. 5 mL of 0.05 M PBS buffer of pH 7 was placed in electrolytic cell and aliquots of 40 to 2000 μL of a glyphosate concentration solution of 20 mg L^{-1} were added. Between each addition of glyphosate, solution was homogenized for 120 s at 1000 r.p.m. Glyphosate quantification was performed by mea-

suring cathodic peak currents difference in the absence and presence of glyphosate ($\delta I = I_t - I_0$; I_t and I_0, the cathodic peak currents with and without glyphosate, respectively).

2.2.2 Spectrophotometric determination

The spectrophotometric analysis of glyphosate was adapted from the methodology described by [28]. This is a colorimetric method, in which a Ruhemann's purple coloured is developed due to the reaction of glyphosate with ninhydrin and sodium molybdate. Standard glyphosate solutions were prepared from a stock solution of 200 mg L^{-1}. In a well-plate, 400 μL glyphosate, 400 μL 2.5% ninhydrin and 400 μL 2.5% sodium molybdate were mixed. The well-plates were then sealed, and the mixtures were heated at a temperature of 90 °C for 8 min, later the samples were cooled to room temperature. The color intensity of samples was measured at 567 nm (λmax) using a UV-Vis spectrophotometer with multi-well plates (Multiskan GO, Thermo Scientific). Finally, the concentration of glyphosate in each sample was determined by using the calibration curve in the range from 5 to 50 mg L^{-1}.

2.3 Adsorption of glyphosate on host materials

The adsorption of glyphosate (Sigma – Aldrich, 90 %) on bentonite and organoclays was carried out using the batch equilibrium method. The host materials (bentonite, OB1, OB1.7 and OB3) were added to 20 mg L^{-1} glyphosate solution at two pHs for adsorption (3 and 10). Adsorption equilibrium experiments were performed using a fixed adsorbent dose of 5 mg in 1.0 mL of glyphosate solution (solid to liquid ratio: 5 g L^{-1}), with initial glyphosate concentrations ranging from 5 to 20 mg L^{-1}. The contact time for all experiments was maintained at 25 minutes under constant stirring. The batch experiment was shaken with an orbital shaker at 300 r.p.m. at 25 °C. The pH was adjusted by adding aliquots of 0.1 M NaOH or 0.1 M HCl. Measurements and experiments were made in triplicate. Electrochemical analytical methods were used to determine the glyphosate concentration at equilibrium. The equation 1 was used to determine the adsorption capacity q_s:

$$q_s = \frac{(C_i - C_e) * V(L)}{m(g)} \tag{1}$$

Where m is the mass of the host materials used, C_i is the initial concentration (mg L^{-1}), C_e is the concentration of the solution at equilibrium (mg L^{-1}), and V is the volume of the aliquot (L). The data obtained in the adsorption study were fitting equilibrium non – linear models to understand the mechanisms and dynamics of the adsorption process (Eq. 2 – 4).

$$\text{Langmuir Isotherm: } q_s = \frac{Q_{\max} K_L C_e}{1 + K_L C_e} \tag{2}$$

$$\text{Freundlich Isotherm: } q_s = K_F C_e^{1/n} \tag{3}$$

$$\text{Sips Isotherm: } q_s = \frac{Q_{\max} K_s C_e^{1/n}}{1 + K_s C_e^{1/n}}, \quad 0 < \frac{1}{n} \leq 1 \tag{4}$$

Where $Q_{(max)}$ is the maximum adsorption capacity (mg g^{-1}), KL is the Langmuir equilibrium constant (L mg^{-1}), KF is the Freundlich equilibrium constant (mg g^{-1} (mg $L^{-1})^{-1/n}$); Ks is the Sips equilibrium constant (mg $L^{-1}1^{-1/n}$, n is the exponent dimensionless [29].

2.4 Encapsulation

Encapsulation was performed based on the methodology of [30] on host materials with better herbicide adsorption behaviour (BG or OBG). 0.1 - 0.4 g of BG or OBG were mixed with 10 mL of 2 % w/v sodium alginate solution for 10 hours at 25 °C and using a magnetic stirrer. The suspensions were introduced in a 10 mL syringe and added through a needle with an internal diameter of 0.45 mm a 6 % w/v calcium chloride solution, stirring constantly for one hour. Bead-shaped encapsulates were dried at 50 °C for 8 h. The encapsulates were named BGE/OBGE(0.1), BGE/OBGE(0.2) and BGE/OBGE(0.4).

Morphology and particle size were investigated with a JEOL JSM 6490 LV scanning electron microscope (SEM). Samples were fixed with conductive carbon adhesive tape and coated with gold using Desk IV DENTON VACUUM sputtering systems. Images were taken at high vacuum with a secondary electron detector. Cross-sectioning of the encapsulates was carried out by freeze-fracture technique. Particle size distribution analysis of the SEM images was carried out with imageJ software. Water Activity (aw) was measured by a *LabSwift-aw* (Novasina, Germany) equipment. Analysis was performed in triplicate at 25 °C.

2.5 Glyphosate Desorption Batch Study

5 mg of glyphosate as BGE or OBGE were added to 1 mL of desionized water in test tubes with constant agitation in an orbital shaker for a time range of 5 minutes to 6 hours at 25 °C. Then, the supernatant was extracted, filtered and the equilibrium concentration in desorption (Ce-D) was determined by UV – Vis spectroscopy. The amount of herbicide remaining after the desorption process ($q_{(e-D)}$) and the percentage of desorption will be calculated considering Eq. 5 and 6, respectively.

$$q_{e-D} = \frac{C_{e-D}}{m} V \tag{5}$$

$$\text{Desorption (\%)} = \left(\frac{q_{e-D}}{q_s}\right) \times 100 \tag{6}$$

Where m is the mass (g) of glyphosate as BGE or OBGE, V supernatant volume (L). The experiments were made for triplicated. The data obtained in the desorption study were fitting kinetics non – linear models to understand the diffusional process (Eq. 7, 8).

$$\text{Korsmeyer–Peppas: } \frac{M_t}{M_\infty} = K_{KP}\, t^n \tag{7}$$

$$\text{Higuchi: } \frac{M_t}{M_\infty} = K_H\, t^{1/2} \tag{8}$$

Where $\frac{M_t}{M_\infty}$ is the fraction of glyphosate released at time t, K_{KP} and K_H are characteristic kinetic constant and n is a diffusional exponent indicating the transport mechanism. Values ≤ 0.5 indicate that the diffusion mechanism is Fickian and if it is between 0.5 - 1.0 it indicates that the diffusion mechanism is non – Fickian or is a mixed chain diffusion and relaxation mechanism [30].

2.6 Soil Column Leaching Experiment

The leaching study of the encapsulated glyphosate was carried out on Pyrex glass soil columns with a 3 cm internal diameter × 25 cm height. The soil used was collected from the natural and ecotourism reserve "La avispa" in Caquetá-Colombia, where the soil has not been treated with any type of pesticide or affected by agricultural activities. The soil was previously characterized (Table S1), dried and sieved. The columns were packed by hand with 128 g of soil from different depths to simulate the soil profile, covering the lower end of the column with cotton and 15 g of river sand. The columns were saturated with distilled water and allowed to drain for 24 hours, then 0.94 mg of glyphosate (from the commercial and encapsulated formulation) were added to reach the recommended dose (4 kg ha^{-1}). After applying the herbicide, the columns were leached daily with 15 mL of distilled water for 11 days, recovering the percolates for filtration and glyphosate quantification by UV-Vis spectroscopy. Three experiments were carried out in soil columns that include the blank (only water), commercial formulation and the formulation of the encapsulated herbicide.

3 Results and discussion

3.1 XRD and FT-IR Analysis of Host Material for Glyphosate

X-ray diffraction of clays are shown in Fig. S1. The precursor clay (Fig. S1a) shows main crystalline phase corresponding to sodium bentonite with an intense 001 reflection at 1.44 nm which corresponds to interlayer hydrated sodium cations [31]. The XRD patterns of bentonite modified with different ratios of hexadecylamonium cations/clay (Fig. S1b - d) are characterized by three set of 001 reflections that correspond to three different basal spaces at 2.85 nm, 3.24 nm and 3.46 nm; these results show an increase in the basal spacing when the amount of hexadecylamonium cations provided is increased due to different conformations of the alkyl chains in the interlayer space, thus, the signal in 2.85 nm (Fig. S1b) is compatible with the double layer conformation and the signals in 3.24 nm (Fig. S1c) and 3.46 nm (Fig. S1d) are compatible with paraffinic conformation [32]. The diffractograms of organobentonites also show reflections with basal gaps between 1.50 nm and 1.69 nm associated with the $d_{001/2}$ plane and indicates a uniform distribution of the laminar charge.

Infrared spectra of bentonite and all synthetized organoclays are compared in Fig. S2. Bentonite (Fig. S2a) shows two bands related to stretching and bending vibration of hydroxyl groups OH^- of water of hydration of interlayer cations in 3480 cm^{-1} and 1640 cm^{-1}, respectively; the band in 3690 cm^{-1} are related to structural hydroxyl groups in the clay. The observed bands in 1028, 520 and 482 cm^{-1} are typical of layered aluminosilicates [33]. The spectra of the organobentonites (Fig. S2b - d) shows the same bands as bentonite and also shows bands related to asymmetric, symmetric and scissoring bending vibrations of methylene groups at 2921, 2854 and 1466 cm^{-1}, respectively [32].

3.2 Glyphosate quantification

Detection and quantification of glyphosate can be carried out by different analytical techniques [34, 35, 36]. For example, UV-Vis spectrophotometry is one of the most widely used techniques [37, 38]. However, analysis comprises a derivatization step with ninhydrin or FMOC-Cl, and a further measurement of the absorbance [39-42]. Thus, electrochemical techniques emerge as an analytical alternative due to their simplicity, low cost, speed, and ability to minimize or eliminate the use of polluting chemicals [43]. The main disadvantage of electrochemical analysis is the poor electroactivity of glyphosate on conventional electrode materials and electrolytic media [44]. Nevertheless, electrode materials such as copper can be used for indirect electrochemical quantification of glyphosate [44–46]. Fig. 1 shows the CVs of a copper electrode in the presence and absence of glyphosate in 0.05 M PBS buffer of pH 7. In the absence of glyphosate (black line), an anodic peak centered at 0.05 V is related to the oxidation of Cu^0 to Cu^{2+}, and a sharp peak in the reverse scan at -0.2 V indicates copper regeneration. On the other hand, the presence of glyphosate in the electrolyte solution changes the electrochemical behavior of the copper electrode (blue line). A decrease in the oxidation and reduction peak currents are observed in the CV with addition of glyphosate, indicating a complexation reaction between Cu^{2+} ions and glyphosate [47, 48].

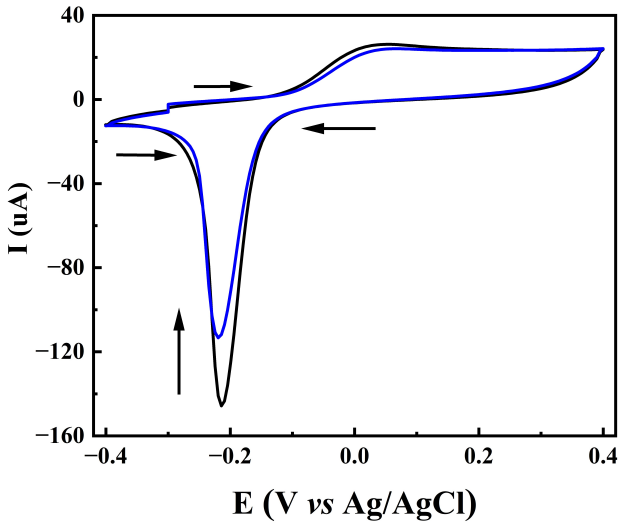

Figure 1: CVs recorded with a Cu electrode in 0.05 M PBS buffer of pH 7 without glyphosate (black line) and with 33.36 mg L^{-1} glyphosate (blue line) at a scan rate of 100 mV s^{-1}.

Based on these results, an electroanalytical method for glyphosate quantification was developed (Fig. 2). Copper electrode performance was evaluated over a 0.1 to 6 mg L^{-1} glyphosate concentrations range (Fig. 2a). A zoom Fig. 2a (inset) shows in more detail cathodic peak current decrease, which is proportional to glyphosate concentration.

A good linear relationship was observed (Fig. 2b). Linear equations can be represented as δI (μA) = 18.972 (mg L^{-1}) + 2.899 (R^2 = 0.948, 0.1 mg $L^{-1} \leq C \leq$ 0.6 mg L^{-1}) and δI (μA) = 5.244 (mg L^{-1}) + 6.965 (R^2 = 0.9995, 0.6 mg $L^{-1} \leq C \leq$ 6 mg L^{-1}). From the two linear segments limit of detection (LOD) and quantification (LOQ) for glyphosate were calculated (Table S2). LOD and LOQ for 0.1 mg $L^{-1} \leq C \leq$ 0.6 mg L^{-1} glyphosate concentration ranges were 0.08 and 0.24 mg L^{-1}, respectively. Quality of the calibration curve at low concentrations of glyphosate is important as a parameter of herbicide quantification in water according to US-EPA guidelines [49].

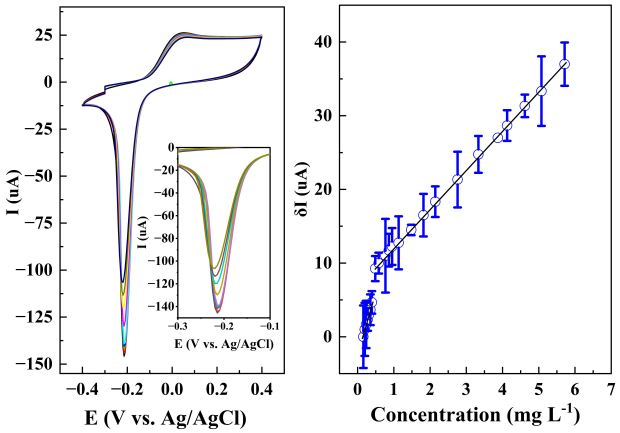

Figure 2: a) CVs recorded with a Cu electrode in 0.05 M PBS buffer of pH 7 for different glyphosate concentrations in the range 0.1 to 6 mg L^{-1}. Scan rate: 100 mV s^{-1} (the inset corresponds to the magnified image of the cathodic peaks); b) Calibration curve corresponding to values of cathodic current decrease as a function of the glyphosate concentration.

On the other hand, during desorption processes of glyphosate from the encapsulates, a limitation in the analysis by CV was observed (Fig. S3). As an example, CV of the BGE(0.2) encapsulated in 0.05 M PBS buffer of pH 7 (Fig, S3, red line). Two characteristics are remarkable with respect at CV without sample (Fig, S3, black line), a shift cathodic peak potential and a lower cathodic peak current. An identical electrochemical behavior was observed when calcium chloride was measured under same analytical conditions (Fig. S3, blue line). These results indicate that calcium ion is an interferant in determination of glyphosate by CV. For this reason, quantification of glyphosate in the desorption process and soil columns leaching was performed by UV-Vis spectroscopy. The LOD and LOQ from the calibration curve are shown in the Table S2.

3.3 Glyphosate Adsorption study

Fig. 3 shows the glyphosate adsorption capacity of bentonite and organobentonites OB1, OB1.7 and OB3 to pH 3 and 10. The bentonite presents a similar adsorption capacity for the two values of pH studied, reaching an adsorption capacity for both of up to 3 mg g^{-1}. At pH 3, the glyphosate is ionized, adopting a positive charge and the edges sites of the clay surface are positively charged and two types of interactions between the glyphosate and surface sites are possible: a weak interaction through outer sphere surface complexes formation or a strong interaction where the glyphosate has a high affinity for the surface through inner sphere surface complexes [50]. Moreover, at pH 10 the glyphosate adopted a negative charged and the edges the clay surface was de-protonated provide strong adsorption sites [51], in this case, the main adsorption mechanism is the interaction of the - O- groups on the edges the clay surface with the -NH_2^+- groups of the glyphosate by electrostatic interaction [52]. The OB1, OB1.7 and OB3 showed a decrease in the adsorption capacity compared to the bentonite studied at pH 3 and 10; this may be related to the competition generated between the ionized glyphosate and the hexadecylammonium cations for the ion exchange sites in the material. The best adsorption capacity of glyphosate in all the organobentonites was at pH 10, due to the fact that at this pH there is an ionic interaction between the negatively ionized glyphosate and the positive surface of the organobentonites as a consequence of the modification with alkylammonium cations [53] and the particular arrangement of the water molecules around the alkyl chains [51, 54].

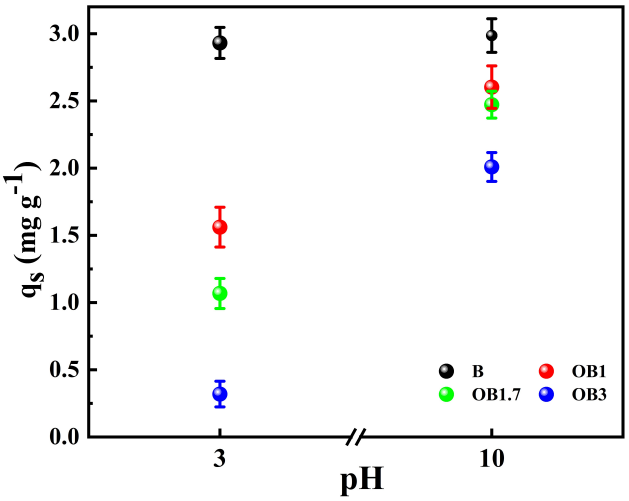

Figure 3: Glyphosate adsorption of bentonite (B) and organobentonites (OB1, OB1.7 and OB3) to pH 3 and 10. Using an initial Glyphosate concentration of 20 mg L^{-1}.

Fig. 4 shows the adsorption isotherms of glyphosate on bentonite and organobentonite at pH 10. The bentonite (Fig. 4a) present a low adsorption capacity at low concentrations, increasing exponentially when the concentration of glyphosate increases, suggesting a cooperative adsorption; while the organobentonites OB1 and OB1.7 (Fig. 4b and c) show consecutive adsorption in successive steps, at low glyphosate concentration the adsorption occur on one kind of site; as the equilibrium glyphosate concentration increased, these sites became saturated and other sites contributed significantly to the adsorption. This behavior is related to heterogeneous surface such as organoclays [55]. The isotherm of OB3 (Fig. 4d) show cooperative adsorption up to saturation point. The adsorption data of all materials were fitted to Langmuir, Fre-

undlich and Langmuir-Freundlich (Sips) models (Table S3); the best fit was with the Sip model, indicating heterogeneity in the adsorption sites on the surface of the materials [56]. The encapsulation step was carried out with those materials host that presented a cooperative adsorption behavior (B and OB3).

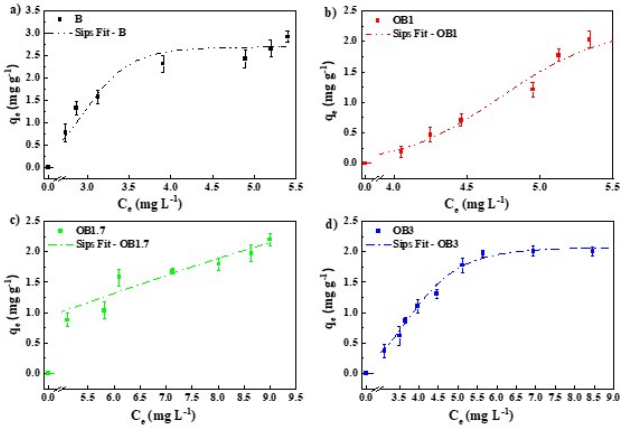

Figure 4: Glyphosate adsorption isotherms and Sips Fit model on bentonite a) B and organobentonites b) OB1; c) OB1.7 and d) OB3. Using an initial Glyphosate concentration (5 – 20 mg L^{-1}) at pH =10.

3.4 Encapsulation

Based on the results of glyphosate adsorption study, bentonite and organobentonite loaded with glyphosate (BG and OBG) were encapsulated. Fig. 5 and S4 shows the organobentonite/glyphosate (OBGE) and bentonite/glyphosate (BGE) encapsulates at different proportions, both before and after the drying process. Prior to drying, the BGE and OBGE beads exhibited a yellowish spherical morphology (characteristic of bentonite), with particle size distributions averaging 2.34 ± 0.08 mm for BGE 0.2, 2.90 ± 0.18 mm for OBGE 0.2, 2.33 ± 0.26 mm for BGE 0.4, and 3.13 ± 0.14 mm for OBGE 0.4 (Fig. 5a and S4c, black). Similar observations have been reported in previous studies using bentonite/alginate encapsulation systems [18, 57]. The larger average particle size of OBGE compared to BGE is attributed to the increased basal spacing caused by the incorporation of hexadecylammonium cations into the organobentonite structure, as supported by X-ray diffraction results. After drying, the encapsulates exhibited a dark brown color (Fig. 5b and S4b), and their average particle size decreased by approximately 60%, yielding values in the range of 1.00 to 1.35 mm (Fig. 5d and S4d, red). This finer fraction was retained between 16 and 18 mesh, and was used for the desorption experiments to ensure sample uniformity. Furthermore, particle size was also observed to vary with changes in the host material-to-alginate ratio, indicating that the inorganic phase significantly influences bead formation and shrinkage behavior during drying.

One of the most important parameters affecting controlled release behavior is the surface of the carrier [57]. SEM images at 60x magnification revealed lower surface roughness of OBGE(0.1) and BGE(0.1) compared to other hot material/alginate ratios. (Fig. 6a and S5a, respectively), this is due to fabrication by extrusion technique [58, 59]. A cross-section shows a shear stress of the encapsulates due to a soft structure (Fig. 6b and S5b), indicating that inside of the encapsulates is not completely dry. However, a rougher and more heterogeneous surface was observed with increasing BGE and OBGE amount, suggesting that the alginate was insufficient to accommodate BGE(0.4) and OBGE(0.4) particles [26]. Furthermore, from these SEM images, it is difficult to distinguish the BGE or OBGE layers in the alginate encapsulates.

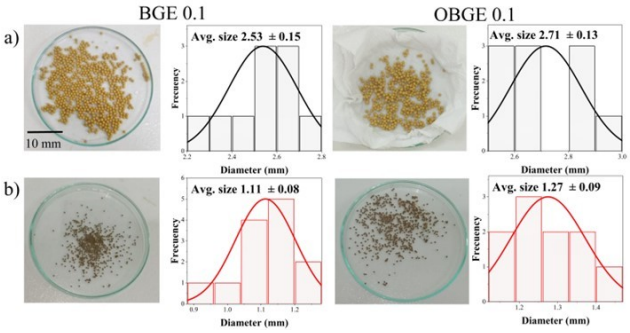

Figure 5: Photographs and particle size distribution bentonite/glyphosate (BGE) or organobentonite/glyphosate (OBGE) encapsulates using 0.1 host material/alginate ratio. a) Before and b) after drying.

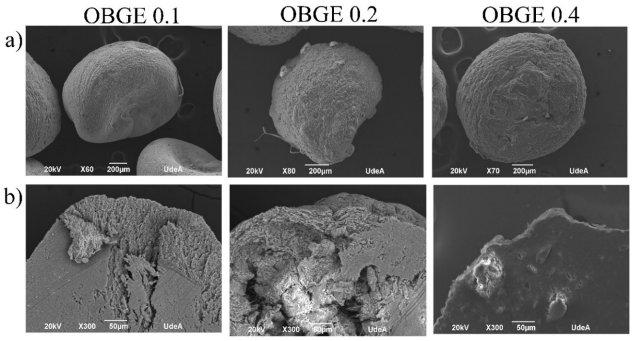

Figure 6: SEM images organobentonite/glyphosate (OBGE) encapsulates using 0.1, 0.2 and 0.4 host material/alginate ratios. a) 60x magnification, b) 300x magnification cross-section of the encapsulates.

The analysis of water activity in bentonite and organobentonite encapsulates with glyphosate allowed us to establish a criterion for determining water availability in the encapsulates, which may either promote or inhibit microbiological growth [60]. Table 1 shows the water activity values of the encapsulates with and without glyphosate. In most cases, the values are below 0.6, suggesting an inhibition of microbial growth [61]. This behavior is common when alginate is used as an encapsulating agent, due to its capacity to protect the active ingredient from degradation [62]. This feature is particularly important when designing controlled-release formulations of glyphosate, since this herbicide tends to be biodegraded by microorganisms into toxic metabolites such as AMPA [63]. In this context, the encapsulation strategy

helps to modulate the availability of the herbicide in the environment, to reduce its immediate biodegradation and the formation of harmful by-products, and to mitigate its ecotoxicological impact on biota.

Encapsulates containing glyphosate also exhibited higher water activity than those without glyphosate, possibly due to the herbicide's strong tendency to hydrate through hydrogen bonding and donor–acceptor interactions between water molecules and its carboxyl and phosphate groups [64]. Among the tested formulations, BGE(0.2) with glyphosate exhibited a water activity above 0.6, which may enable microbial growth and therefore represent a limitation during agricultural application. For the release experiments, the selected encapsulates were BGE/OBGE(0.1) and BGE/OBGE(0.4), both of which maintained water activity levels below 0.6.

Table 1: Water activity of encapsulates with and without glyphosate

	Water activity*	
Encapsulate	**With Glyphosate**	**Without Glyphosate**
BGE (0.4)	0.542	0.468
BGE (0.2)	0.648	0.662
BGE (0.1)	0.535	0.375
OBGE (0.4)	0.489	0.389
OBGE (0.2)	0.340	0.512
OBGE (0.1)	0.483	0.402

*Water activity < 0.6 growth of microorganisms inhibited

3.5 Release profile of glyphosate encapsulated in water

Fig. 7a shows the cumulative desorption of BGE/OBGE(0.1) and BGE/OBGE(0.4) encapsulates. These formulations showed a rapid release profile in the first hour, reaching a release between 25 – 35 %. Complete release was not reached in the time range evaluated in the experiment. The organobentonite encapsulates OBGE(0.1) and OBGE(0.4) presented a decrease in the release rate of the herbicide compared to the bentonite encapsulates BGE(0.1) and BGE(0.4); due to the influence of the matrix that supports glyphosate, where there are stronger interactions between glyphosate -organobentonite, compared to the glyphosate - bentonite interaction where the diffusion process is favored. The OBGE(0.1) encapsulate presents a slower release in water than the OBGE(0.4) encapsulate, a similar behavior is observed for the BGE bentonite encapsulates. This behavior is related with the amount of alginate provided in the encapsulation (0.2 g of alginate was provided in all encapsulates) which physically entraps the glyphosate-incorporated clay/organoclay and controls the diffusion of the herbicide outside of alginate beads. The data were fitted to the Korsmeyer-Peppas and Higuchi kinetic models (Fig. 7b – e) which are related to controlled release profiles whose predominant mechanism is simple Fickian diffusion [30].

The data showed a better fit to the Korsmeyer–Peppas model than to the Higuchi model, as indicated by the determination coefficients (R^2) presented in Table 2. To provide a more robust and comprehensive evaluation of model performance, additional statistical parameters were included in the table, specifically the adjusted coefficient of determination (Adj R^2) and the standard error of estimate (SEE). These metrics further support the adequacy of the Korsmeyer–Peppas model in describing the release kinetics of glyphosate from the encapsulated systems. This fitting suggests that water penetrating the polymer matrix governs the release of the herbicide. Supporting this interpretation are the values of the diffusion exponent n derived from the Korsmeyer–Peppas model, all of which are ≤ 0.5. This indicates that the release mechanism follows a Fickian diffusion process, where the active ingredient diffuses outward at a rate primarily controlled by the balance between diffusion and polymer relaxation [65]. Additionally, the kinetic constant K of the Korsmeyer–Peppas model indicates that glyphosate encapsulated in organoclay matrices is released more slowly than from bentonite-based encapsulates. Based on these results, the OBGE(0.1) formulation was selected for the soil column leaching experiments.

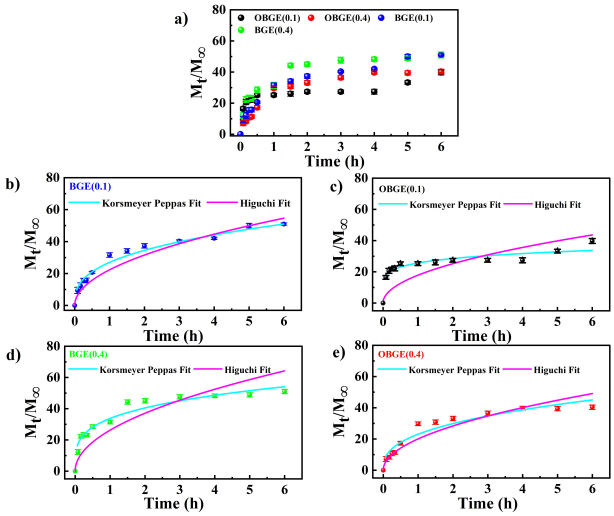

Figure 7: Release behavior of glyphosate encapsulate a) Cumulative release of glyphosate in water and Korsmeyer and Peppas and Higuchi model Fit of b) BGE(0.1); c) OBGE(0.1); d)BGE(0.4) and e)OBGE(0.4).

3.6 Release profile of glyphosate encapsulated in soil columns

The glyphosate leaching curves in the soil columns (Fig. 8) indicate that the encapsulated formulation slowly releases the active ingredient, reaching up to approximately 38% leaching after the addition of 90 mL of cumulative eluent, while the commercial formulation released nearly 90% of glyphosate after 145 mL. In both cases, the release occurs in two steps: an initial slow-release step followed by a dynamic equilibrium between the adsorption and desorption processes in the soil [66]. The leaching tests confirmed that the encapsulated system significantly reduces glyphosate mobility, delaying its vertical transport through the soil profile and demonstrating potential for minimizing contamination of deeper soil layers and groundwater. However, it is important to critically assess the agronomic implications of releasing only ~38% of the herbicide. Although slow and localized release is beneficial to reduce off-target losses and environmental impact [67, 68], it is equally important to ensure that an adequate amount of active ingredient is eventually released to achieve effective

Table 2: Kinetic parameters of Korsmeyer – Peppas and Higuchi model.

Kinetic Model	Parameter	BGE (0.1)	BGE (0.4)	OBGE (0.1)	OBGE (0.4)
Korsmeyer–Peppas	n	0.355 ± 0.020	0.303 ± 0.026	0.153 ± 0.002	0.373 ± 0.043
	$K_{K\text{-}P}$	26.967 ± 0.772	33.721 ± 1.106	25.611 ± 0.024	23.039 ± 1.324
	R^2	0.980	0.938	0.813	0.922
	Adj R^2	0.967	0.897	0.688	0.870
	SEE	0.071	0.125	0.216	0.139
Higuchi	K_H	22.306 ± 0.712	26.207 ± 1.854	17.791 ± 1.854	20.038 ± 1.002
	R^2	0.935	0.744	0.042	0.904
	Adj R^2	0.892	0.573	−0.597	0.840
	SEE	0.127	0.252	0.489	0.155

$K_{(K-P)}$= Korsmeyer—Peppas constant, K_H= Higuchi dissolution constant, n= Diffusional exponent.

weed control. In this formulation, approximately 60% of the glyphosate remains retained, which may raise concerns about whether the encapsulation system releases a sufficient dose over a relevant agronomic timeframe.

In this context, it has been suggested that encapsulation systems should ideally release between 60–80% of the active ingredient to balance efficacy and environmental safety [69, 70]. Therefore, although the tested OBGE(0.1) formulation successfully limits leaching, it may require further optimization to enhance long-term release while preserving its controlled-release behavior. Strategies such as adjusting the polymer-to-host material ratio, modifying crosslinking density, or integrating pH-sensitive components could help improve the release efficiency without compromising the environmental advantages.

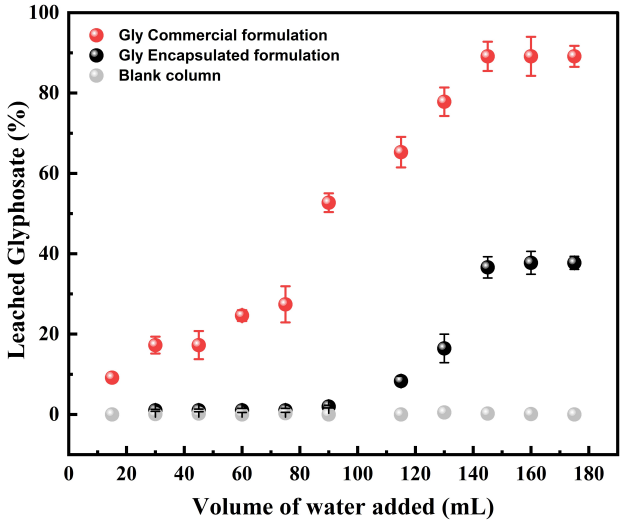

Figure 8: Glyphosate leaching curves in the encapsulated formulation (red square), commercial formulation (black square) and blank column (gray square).

4 Conclusions

Glyphosate-controlled release formulations were obtained by incorporating the organophosphorus herbicide into organobentonite (host material) followed by encapsulation with alginate. The adsorption mechanism of glyphosate onto organoclay at pH 10 involves ionic interactions between the negatively charged glyphosate species and the positively charged surface of the organobentonites, resulting from modification with alkylammonium cations. This process is also influenced by the specific arrangement of water molecules around the alkyl chains and the heterogeneity of adsorption sites on the surface of the materials.

The encapsulates exhibited spherical shapes larger than 2.3 mm and water activity values below the threshold for microbial growth, which is an important consideration in the design of controlled-release systems. This is particularly relevant for glyphosate, as it can be biodegraded by soil bacteria into secondary metabolites such as AMPA, which are more persistent and potentially harmful to the environment.

Desorption experiments in water revealed that the use of organobentonite as a support material significantly reduced the release rate of glyphosate compared to bentonite. This behavior was also influenced by the amount of alginate used in the encapsulation process, which physically entraps the glyphosate-loaded clay or organoclay and modulates herbicide diffusion from the beads. The release data fitted well to empirical models, indicating a Fickian diffusion-controlled process.

Soil column experiments demonstrated that the encapsulated glyphosate formulation was released more slowly and in sequential steps compared to the commercial formulation, thereby limiting vertical mobility through the soil profile.

The findings of this study highlight the potential of this controlled-release system to improve the environmental behavior of glyphosate. While encapsulation may contribute to more localized and gradual release, reducing the risk of leaching, the possible formation of persistent degradation products such as AMPA must be considered. Therefore, although this strategy shows promise for supporting more sustainable agricultural practices, especially in ecologically sensitive regions such as the Colombian Amazon, further evaluation under field conditions is needed to fully assess its environmental implications.

Acknowledgements and Funding

Dr. Ruiz thanks the Ministerio de Ciencia y Tecnología, MINCIENCIAS, Colombia, for a grant “Beca excelencia doctoral 2019”.

Authors Conflicts of Interest

The authors declare no competing financial interest.

References

[1] B. Ciasca *et al.*, "Rapid and reliable detection of glyphosate in pome fruits, berries, pulses and cereals by flow injection – Mass spectrometry," Food Chem., vol. 310, p. 125813, 2020, doi: 10.1016/j.foodchem.2019.125813.

[2] A. Scherner, L. Avila, F. Schreiber, N. D. Kruse, J. A. Fernando, and É. N. Garcia, "Susceptibility of peruvian watergrass and rice cutgrass to glyphosate under soil moisture variations," Crop Prot., vol. 98, pp. 1–7, 2017, doi: 10.1016/j.cropro.2017.03.003.

[3] D. Hurtado and I. Vélez-Torres, "Toxic dispossession: on the social impacts of the aerial use of glyphosate by the sugarcane agroindustry in Colombia," Crit. Criminol., vol. 28, no. 4, pp. 557–576, 2020.

[4] D. Valbuena, M. Cely-Santos, and D. Obregón, "Agrochemical pesticide production, trade, and hazard: Narrowing the information gap in Colombia," J. Environ. Manage., vol. 286, p. 112141, 2021.

[5] G. Basílico, M. Cogollo-Rueda, V. Ionno, A. Faggi, and L. de Cabo, "The Use of Glyphosate in Regions of Argentina and Colombia and Its Socio-Environmental Impacts," Agrochem. Soil Environ. Impacts Remediat., pp. 195–212, Jan. 2022, doi: 10.1007/978-981-16-9310-6_9.

[6] I. R. Herrera and J. Dessein, "'We are not Drug Traffickers, We are Colombian Peasants': The voices and history of cocaleros in the substitution programme of illicit crops in Colombia," Geoforum, vol. 141, p. 103734, 2023.

[7] K. Z. Guyton *et al.*, "Carcinogenicity of tetrachlorvinphos, parathion, malathion, diazinon, and glyphosate," Lancet Oncol., vol. 16, no. 5, pp. 490–491, 2015.

[8] C. Acero and F. Thomson, "'Everything peasants do is illegal': Colombian coca growers' everyday experiences of law enforcement and its impacts on state legitimacy," Third World Q., vol. 43, no. 11, pp. 2674–2692, 2022.

[9] L. C. Reyes, "Estimating the causal effect of forced eradication on coca cultivation in Colombian municipalities," World Dev., vol. 61, pp. 70–84, 2014.

[10] R. Kanissery, B. Gairhe, D. Kadyampakeni, O. Batuman, and F. Alferez, "Glyphosate: Its environmental persistence and impact on crop health and nutrition," Plants, vol. 8, no. 11, pp. 1–11, 2019, doi: 10.3390/plants8110499.

[11] S. Klátyik *et al.*, "Terrestrial ecotoxicity of glyphosate, its formulations, and co-formulants: evidence from 2010–2023," Environ. Sci. Eur., vol. 35, no. 1, pp. 1–29, 2023.

[12] V. F. Lutri *et al.*, "Hydrogeological features affecting spatial distribution of glyphosate and AMPA in groundwater and surface water in an agroecosystem.," Sci. Total Environ., vol. 711, p. 134557, 2020, doi: 10.1016/j.scitotenv.2019.134557.

[13] S. Bott *et al.*, "Phytotoxicity of glyphosate soil residues re-mobilised by phosphate fertilisation," Plant Soil, vol. 342, no. 1–2, pp. 249–263, 2011, doi: 10.1007/s11104-010-0689-3.

[14] S. J. Trenfield and A. W. Basit, Modified drug release: Current strategies and novel technologies for oral drug delivery. Elsevier Inc., 2020. doi: 10.1016/B978-0-12-818038-9.00006-5.

[15] H. El-hamshary, M. H. El-newehy, M. Mohideen, A. El-faham, and A. S. Elsherbiny, "Evaluation of clay-ionene nanocomposite carriers for controlled drug delivery: synthesis, in vitro drug release, and kinetics," Mater. Chem. Phys., pp. 122–132, 2019, doi: 10.1016/j.matchemphys.2018.12.054.

[16] Q. Tang *et al.*, "Medium-chain triglyceride/water Pickering emulsion stabilized by phosphatidylcholine-kaolinite for encapsulation and controlled release of curcumin," Colloids Surfaces B Biointerfaces, vol. 183, p. 110414, 2019.

[17] K. Hnana, A. Barhoun, and K. Draoui, "Improvement of glyphosate adsorption using new composites based on ghassoul and chitosan: Kinetics and equilibrium study," Mediterr. J. Chem., vol. 9, no. 4, pp. 266–279, 2019, doi: 10.13171/MJC9419111121087KD.

[18] D. Garmia, H. Zaghouane-Boudiaf, and C. V. Ibbora, "Preparation and characterization of new low cost adsorbent beads based on activated bentonite encapsulated with calcium alginate for removal of 2,4-dichlorophenol from aqueous medium," Int. J. Biol. Macromol., vol. 115, pp. 257–265, 2018, doi: 10.1016/j.ijbiomac.2018.04.064.

[19] A. Berardi, L. Bisharat, M. Cespi, I. A. Basheti, L. Pavoni, and H. S. Alkhatib, "Controlled release properties of zein powder filled into hard gelatin capsules," Powder Technol., pp. 703–713, 2017, doi: 10.1016/j.powtec.2017.07.093.

[20] X. L. Chen, F. Li, H. Y. Chen, H. J. Wang, and G. G. Li, "Fe2O3/TiO2 functionalized biochar as a heterogeneous catalyst for dyes degradation in water under Fenton processes," J. Environ. Chem. Eng., vol. 8, no. 4, p. 103905, 2020, doi: 10.1016/j.jece.2020.103905.

[21] J. Wu, Z. Zhang, W. Zhou, X. Liang, and G. Zhou, "Mechanism of a long-term controlled drug release system based on simple blended electrospun fibers," J. Control. Release, vol. 320, no. December 2019, pp. 337–346, 2020, doi: 10.1016/j.jconrel.2020.01.020.

[22] M. Jinhong, Z. Hui, D. G. Evans, and D. Xue, "Novel-layered pesticide slow/controlled release materials-supramolecular structure and slow release property of glyphosate intercalated layered double hydroxides," vol. 50, no. 8, pp. 745–751, 2005.

[23] N. T. K. Phuong, H. N. N. Ha, N. T. P. Dieu, and B. T. Huy, "Herbicide/Zn-Al-layered double hydroxide hybrid composite: synthesis and slow/controlled release properties," Environ. Sci. Pollut. Res., vol. 24, no. 23, pp. 19386–19392, 2017, doi: 10.1007/s11356-017-9580-6.

[24] A. Gupta and D. K. Sharma, "Thermal-Degradation Kinetics of Neem-Alginate-Clay Based Controlled Pesticide Release Formulations," Int. J. Res. Environ. Sci., vol. 3, no. 4, pp. 17–23, 2017, doi: 10.20431/2454-9444.0304003.

[25] W. H. Yu, T. T. Zhu, D. S. Tong, M. Wang, Q. Q. Wu, and C. H. Zhou, "Preparation of organo-montmorillonites and the relationship between microstructure and swellability," Clays Clay Miner., vol. 65, no. 6, pp. 417–430, 2017, doi: 10.1346/CCMN.2017.064068.

[26] H. Zhang, Y. Shi, X. Xu, M. Zhang, and L. Ma, "Structure Regulation of Bentonite-Alginate Nanocomposites for Controlled Release of Imidacloprid," ACS Omega, vol. 5, p. 10068-10076, 2020, doi: 10.1021/acsomega.0c00610.

[27] M. C. Pazos, L. R. Bravo, S. E. Ramos, F. J. Osuna, E. Pavón, and M. D. Alba, "Multiple pollutants removal by functionalized heterostructures based on Na-2-Mica," Appl. Clay Sci., vol. 196, p. 105749, Oct. 2020, doi: 10.1016/J.CLAY.2020.105749.

[28] J. P. K. Gill, N. Sethi, and A. Mohan, "Analysis of the glyphosate herbicide in water, soil and food using derivatising agents," Environ. Chem. Lett., vol. 15, no. 1, pp. 85–100, 2017, doi: 10.1007/s10311-016-0585-z.

[29] É. C. Lima, M. A. Adebayo, and F. M. Machado, "Kinetic and equilibrium models of adsorption," Carbon Nanostructures, vol. 0, no. 9783319188744, pp. 33–69, 2015, doi: 10.1007/978-3-319-18875-1_3.

[30] A. Rashidzadeh, A. Olad, and M. Jalil Hejazi, "Controlled Release Systems Based on Intercalated Paraquat onto Montmorillonite and Clinoptilolite Clays Encapsulated with Sodium Alginate," 2015, doi: 10.1002/adv.21597.

[31] A. Oussalah, A. Boukerroui, A. Aichour, and B. Djellouli, "Cationic and anionic dyes removal by low-cost hybrid alginate/natural bentonite composite beads: Adsorption and reusability studies," Int. J. Biol. Macromol., vol. 124, pp. 854–862, 2018, doi: 10.1016/j.ijbiomac.2018.11.197.

[32] Y. Li and H. Ishida, "Concentration-dependent conformation of alkyl tail in the nanoconfined space: Hexadecylamine in the silicate galleries," Langmuir, vol. 19, no. 6, pp. 2479–2484, 2003, doi: 10.1021/la026481c.

[33] S. Yang, M. Gao, Z. Luo, and Q. Yang, "The characterization of organo-montmorillonite modified with a novel aromatic-containing gemini surfactant and its comparative adsorption for 2-naphthol and phenol," Chem. Eng. J., vol. 268, pp. 125–134, 2015, doi: 10.1016/j.cej.2015.01.060.

[34] K. Kocadal, F. B. Alkas, D. Battal, and S. Saygi, "A review on advances and perspectives of glyphosate determination: challenges and opportunities," Arch. Environ. Prot., vol. 48, no. 3, pp. 89–98, 2022, doi: 10.24425/aep.2022.142693.

[35] K. Melo, D. Nucci, A. Trape, and P. Pires-Rosa, "Brief review analytical methods for the determination of glyphosate," MOJ Toxicol., vol. 4, no. 1, pp. 39–42, 2018, doi: 10.15406/mojt.2018.04.00088.

[36] A. L. Valle, F. C. C. Mello, R. P. Alves-Balvedi, L. P. Rodrigues, and L. R. Goulart, "Glyphosate detection: methods, needs and challenges," Environ. Chem. Lett., vol. 17, no. 1, pp. 291–317, 2019, doi: 10.1007/s10311-018-0789-5.

[37] M. L.C. Passos and M. L. M.F.S. Saraiva, "Detection in UV-visible spectrophotometry: Detectors, detection systems, and detection strategies," Meas. J. Int. Meas. Confed., vol. 135, pp. 896–904, 2019, doi: 10.1016/j.measurement.2018.12.045.

[38] C. V. Waiman, M. J. Avena, M. Garrido, B. Fernández Band, and G. P. Zanini, "A simple and rapid spectrophotometric method to quantify the herbicide glyphosate in aqueous media. Application to adsorption isotherms on soils and goethite," Geoderma, vol. 170, pp. 154–158, 2012, doi: 10.1016/j.geoderma.2011.11.027.

[39] J. C. Diel *et al.*, "Carbon nanotubes impregnated with metallic nanoparticles and their application as an adsorbent for the glyphosate removal in an aqueous matrix," J. Environ. Chem. Eng., vol. 9, no. 2, 2021, doi: 10.1016/j.jece.2021.105178.

[40] D. E. Felton, M. Ederer, T. Steffens, P. L. Hartzell, and K. V. Waynant, "UV-Vis Spectrophotometric Analysis and Quantification of Glyphosate for an Interdisciplinary Undergraduate Laboratory," J. Chem. Educ., vol. 95, no. 1, pp. 136–140, 2018, doi: 10.1021/acs.jchemed.7b00440.

[41] P. Gros, A. A. Ahmed, O. Kühn, and P. Leinweber, "Influence of metal ions on glyphosate detection by FMOC-Cl," Environ. Monit. Assess., vol. 191, no. 4, pp. 1–12, 2019, doi: 10.1007/s10661-019-7387-2.

[42] M. Russo, G. Iervolino, and V. Vaiano, "W-doped zno photocatalyst for the degradation of glyphosate in aqueous solution," Catalysts, vol. 11, no. 234, pp. 1–18, 2021, doi: 10.3390/catal11020234.

[43] L. A. Zambrano-intriago, C. G. Amorim, J. M. Rodríguez-díaz, A. N. Araújo, and M. C. B. S. M. Montenegro, "Challenges in the design of electrochemical sensor for glyphosate-based on new materials and biological recognition," Sci. Total Environ., vol. 793, no. 148496, pp. 1–17, 2021, doi: 10.1016/j.scitotenv.2021.148496.

[44] J. S. Noori, J. Mortensen, and A. Geto, "Recent development on the electrochemical detection of selected pesticides: A focused review," Sensors (Switzerland), vol. 20, no. 8, 2020, doi: 10.3390/s20082221.

[45] S. Pintado, M. R. Montoya, R. Rodríguez-Amaro, M. Mayén, and J. M. R. Mellado, "Electrochemical determination of glyphosate in waters using electrogenerated copper ions," Int. J. Electrochem. Sci., vol. 7, no. 3, pp. 2523–2530, 2012.

[46] M. Regiart *et al.*, "An Electrochemically Synthesized Nanoporous Copper Microsensor for Highly Sensitive and Selective Determination of Glyphosate," ChemElectroChem, vol. 7, no. 7. pp. 1558–1566, 2020. doi: 10.1002/celc.202000064.

[47] D. W. Sun, L. Huang, H. Pu, and J. Ma, "Introducing reticular chemistry into agrochemistry," Chem. Soc. Rev., vol. 50, no. 2, pp. 1070–1110, Feb. 2021, doi: 10.1039/C9CS00829B.

[48] W. Zhang *et al.*, "A method for determining glyphosate and its metabolite aminomethyl phosphonic acid by gas chromatography-flame photometric detection," J. Chromatogr. A, vol. 1589, pp. 116–121, 2019, doi: 10.1016/j.chroma.2018.12.039.

[49] U.S. Environmental Protection Agency, "National Primary Drinking Water Regulations," 2022.

[50] G. A. Khoury, T. C. Gehris, L. Tribe, R. M. Torres Sánchez, and M. dos Santos Afonso, "Glyphosate adsorption on montmorillonite: An experimental and theoretical study of surface complexes," Appl. Clay Sci., vol. 50, no. 2, pp. 167–175, 2010, doi: 10.1016/j.clay.2010.07.018.

[51] G. Lagaly, M. Ogawa, and I. Dékány, "Clay Mineral–Organic Interactions," Dev. Clay Sci., vol. 5, pp. 435–505, Jan. 2013, doi: 10.1016/B978-0-08-098258-8.00015-8.

[52] S. Besghaier *et al.*, "Glyphosate adsorption onto porous clay heterostructure (PCH): kinetic and thermodynamic studies," Brazilian J. Chem. Eng., no. 0123456789, 2021, doi: 10.1007/s43153-021-00166-7.

[53] S. Y. Martinez Stagnaro and C. Volzone, "Adsorption of anionic dyes monoazo and diazo using organobentonites," SN Appl. Sci., vol. 1, no. 1, 2019, doi: 10.1007/s42452-018-0070-3.

[54] R. Guégan, "Organoclay applications and limits in the environment," Comptes Rendus Chim., vol. 22, no. 2–3, pp. 132–141, Feb. 2019, doi: 10.1016/J.CRCI.2018.09.004.

[55] F. Bergaya, B. K. G. Theng, and G. Lagaly, "Chapter 11 Clays, Environment and Health," Dev. Clay Sci., 2006, doi: 10.1016/S1572-4352(05)01019-6.

[56] D. D. Do, Adsorption analysis: Equilibria and kinetics (with cd containing computer MATLAB programs), vol. 2. World Scientific, 1998.

[57] L. Zhang, C. Chen, G. Zhang, B. Liu, Z. Wu, and D. Cai, "Electrical-Driven Release and Migration of Herbicide Using a Gel-Based Nanocomposite," J. Agric. Food Chem., vol. 68, no. 6, pp. 1536–1545, 2020, doi: 10.1021/acs.jafc.9b07166.

[58] B. B. Lee, P. Ravindra, and E. S. Chan, "Size and shape of calcium alginate beads produced by extrusion dripping," Chem. Eng. Technol., vol. 36, no. 10, pp. 1627–1642, 2013, doi: 10.1002/ceat.201300230.

[59] N. T. T. Uyen, Z. A. A. Hamid, N. X. T. Tram, and N. Ahmad, "Fabrication of alginate microspheres for drug delivery: A review," Int. J. Biol. Macromol., vol. 153, pp. 1035–1046, 2020, doi: 10.1016/j.ijbiomac.2019.10.233.

[60] M. de A. Etchepare *et al.*, "Microencapsulação de probióticos utilizando alginato de sódio," Cienc. Rural, vol. 45, no. 7, pp. 1319–1326, 2015, doi: 10.1590/0103-8478cr20140938.

[61] A. J. Fontana, "Minimum Water Activity Limits for Growth of Microorganisms," Water Act. Foods, pp. 571–572, 2020, doi: 10.1002/9781118765982.app4.

[62] M. A. S. Santos and M. T. C. Machado, "Coated alginate–chitosan particles to improve the stability of probiotic yeast," Int. J. Food Sci. Technol., vol. 56, no. 5, pp. 2122–2131, 2021, doi: 10.1111/ijfs.14829.

[63] D. Feng, A. Soric, and O. Boutin, "Treatment technologies and degradation pathways of glyphosate: A critical review," Sci. Total Environ., vol. 742, p. 140559, 2020, doi: 10.1016/j.scitotenv.2020.140559.

[64] O. Fliss, K. Essalah, and A. Ben Fredj, "Stabilization of glyphosate zwitterions and conformational/tautomerism mechanism in aqueous solution: insights from ab initio and density functional theory-continuum model calculations," Phys. Chem. Chem. Phys., vol. 23, no. 46, pp. 26306–26323, Dec. 2021, doi: 10.1039/D1CP03161A.

[65] Y. Fu and W. J. Kao, "Drug release kinetics and transport mechanisms of non-degradable and degradable polymeric delivery systems", vol. 7, no. 4, pp. 429–444, Apr. 2010, doi: 10.1517/17425241003602259.

[66] T. Katagi, "Soil column leaching of pesticides," Rev. Environ. Contam. Toxicol., vol. 221, pp. 1–105, 2013, doi: 10.1007/978-1-4614-4448-0_1

[67] J. K. Patra *et al.*, "Nano based drug delivery systems: recent developments and future prospects," J. Nanobiotechnology 2018 161, vol. 16, no. 1, pp. 1–33, Sep. 2018, doi: 10.1186/S12951-018-0392-8.

[68] P. Fincheira *et al.*, "Eco-efficient systems based on nanocarriers for the controlled release of fertilizers and pesticides: Toward smart agriculture," Nanomaterials, vol. 13, no. 13, p. 1978, 2023.

[69] T. O. Machado, J. Grabow, C. Sayer, P. H. H. de Araújo, M. L. Ehrenhard, and F. R. Wurm, "Biopolymer-based nanocarriers for sustained release of agrochemicals: A review on materials and social science perspectives for a sustainable future of agri-and horticulture," Adv. Colloid Interface Sci., vol. 303, p. 102645, 2022.

[70] C. An *et al.*, "Nanomaterials and nanotechnology for the delivery of agrochemicals: strategies towards sustainable agriculture," J. Nanobiotechnology, vol. 20, no. 1, p. 11, 2022.

Supplementary Material
Supplementary Figures

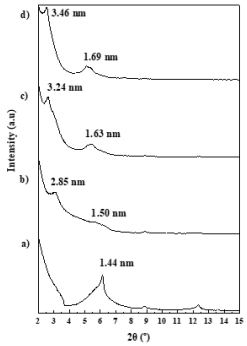

Figure S1: Glyphosate leaching curves in the encapsulated formulation (red square), commercial formulation (black square) and blank column (gray square).

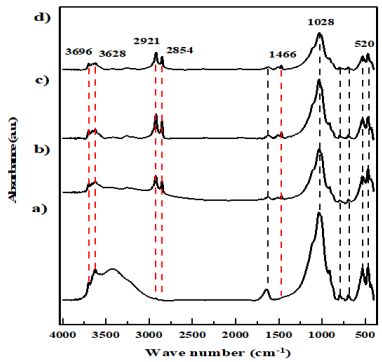

Figure S2: IR spectra of a) bentonite and organobentonites modified with hexadecylamonium cations b) OB1, c) OB1.7 and d) OB3.

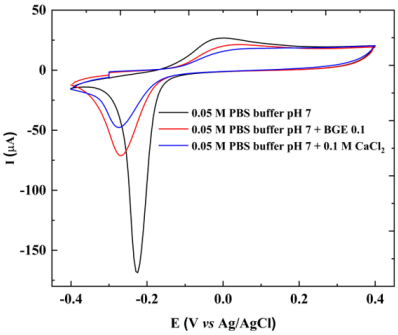

Figure S3: CVs recorded with a Cu electrode. Scan rate: 100 mV s^{-1}.

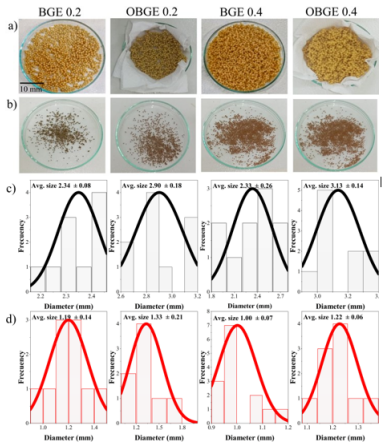

Figure S4: Photographs and particle size distribution bentonite/glyphosate (BGE) or organobentonite/glyphosate (OBGE) encapsulates using 0.2 and 0.4 host material/alginate ratio. a, c) Before and b, d) after drying.

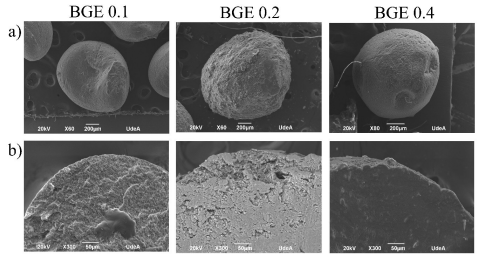

Figure S5: SEM images bentonite/glyphosate (BGE) encapsulates using 0.1, 0.2 and 0.4 host material/alginate ratios. a) 60x magnification, b) 300x magnification cross-section of the encapsulates.

Supplementary Tables

Table S1: Main properties of the soil used in this work.

Soil depth (cm)	Clay (%)	Sand (%)	OM* (%)	pH
0–20	24	73	20	4.2
20–40	28	67	17	4.7
40–60	33	63	12	4.2
60–80	33	59	9	4.5

*OM: Organic matter.

Table S2: LOD and LOQ of the calibration curve for glyphosate quantification.

Analytical technique	Concentration range (mg L^{-1})	LOD (mg L^{-1})	LOQ (mg L^{-1})
Electrochemical	$0.1 \leq C \leq 0.6$	0.08	0.24
	$0.6 \leq C \leq 6$	0.22	0.69
Spectrophotometric	$5 \leq C \leq 50$	0.14	0.46

Table S3: Fit of the glyphosate adsorption isotherms results with nonlinear models for bentonite and organobentonites.

Adsorbent	Model	R^2	Isotherm parameters		
			Q_{max} (mg g^{-1})	K	n
B	Langmuir	0.839	5.450×10^4	8.818×10^{-10}	–
	Freundlich	0.910	–	0.220	1.337
	Sips	0.964	2.696 ± 0.138	0.332 ± 0.008	11.481 ± 2.852
OB1	Langmuir	0.662	2.006×10^4	1.372×10^{-5}	–
	Freundlich	0.819	–	0.043	2.046
	Sips	0.971	2.331 ± 0.097	0.210 ± 0.003	13.289 ± 2.109
OB1.7	Langmuir	–	–	–	–
	Freundlich	0.960	–	0.111 ± 0.026	1.361 ± 0.118
	Sips	0.968	4.974 ± 3.54	0.096 ± 0.069	1.846 ± 0.512
OB3	Langmuir	0.829	9.407	3.336×10^{-2}	–
	Freundlich	0.818	–	0.325	0.875
	Sips	0.986	2.078 ± 0.053	0.257 ± 0.004	6.323 ± 0.720

K: Langmuir (L mg^{-1}), Freundlich (mg g^{-1})(L mg^{-1})^n and Sips (L mg^{-1})^n adsorption constant; n: adsorption intensity; Q_{max}: maximum calculated adsorption capacity.